Odd Diffusivity of Chiral Random Motion (Appendix)

Cory Hargus,[1] Jeffrey M. Epstein,[2] and Kranthi K. Mandadapu[1,3]

[1] *Department of Chemical and Biomolecular Engineering, University of California, Berkeley, CA, USA*
[2] *Department of Physics, University of California, Berkeley, CA, USA*
[3] *Chemical Sciences Division, Lawrence Berkeley National Laboratory, Berkeley, CA, USA*

A.1. CHIRAL RANDOM WALK

In this appendix, we present derivations of the analytical expressions in the main text concerning the chiral random walk model. We begin by considering the balance equations for the joint probability densities of the particle occupying coordinates (x, y) at time t while moving in one of the four available directions indicated by $\{\rightarrow, \uparrow, \leftarrow, \downarrow\}$ with fixed speed v_0. For instance,

$$\begin{aligned} P_{\rightarrow}(x,y,t+\delta t) = P_{\rightarrow}(x-\delta x,y,t) + \delta t\big[&\Gamma_1 P_{\downarrow}(x,y,t) + \Gamma_2 P_{\leftarrow}(x,y,t) \\ &+\Gamma_3 P_{\uparrow}(x,y,t) - \gamma P_{\rightarrow}(x,y,t)\big]\,, \end{aligned} \tag{A.1}$$

where $\delta x = v_0 \delta t$ and $\gamma = \Gamma_1 + \Gamma_2 + \Gamma_3$ is the total turning frequency. Taking the limit $\delta t \to 0$ and repeating the process for the other directions yields the coupled master equations (15)-(18). We can solve the master equations by applying Fourier and Laplace transforms in space and time, respectively:

$$(s+\gamma)\tilde{P}_{\rightarrow}(\boldsymbol{k},s) + \mathrm{i}k_x v_0 \tilde{P}_{\rightarrow}(\boldsymbol{k},s) - \Gamma_1 \tilde{P}_{\downarrow}(\boldsymbol{k},s) - \Gamma_2 \tilde{P}_{\leftarrow}(\boldsymbol{k},s) - \Gamma_3 \tilde{P}_{\uparrow}(\boldsymbol{k},s) = P_{\rightarrow}(\boldsymbol{k},0)\,, \tag{A.2}$$

$$(s+\gamma)\tilde{P}_{\uparrow}(\boldsymbol{k},s) + \mathrm{i}k_y v_0 \tilde{P}_{\uparrow}(\boldsymbol{k},s) - \Gamma_1 \tilde{P}_{\rightarrow}(\boldsymbol{k},s) - \Gamma_2 \tilde{P}_{\downarrow}(\boldsymbol{k},s) - \Gamma_3 \tilde{P}_{\leftarrow}(\boldsymbol{k},s) = P_{\uparrow}(\boldsymbol{k},0)\,, \tag{A.3}$$

$$(s+\gamma)\tilde{P}_{\leftarrow}(\boldsymbol{k},s) - \mathrm{i}k_x v_0 \tilde{P}_{\leftarrow}(\boldsymbol{k},s) - \Gamma_1 \tilde{P}_{\uparrow}(\boldsymbol{k},s) - \Gamma_2 \tilde{P}_{\rightarrow}(\boldsymbol{k},s) - \Gamma_3 \tilde{P}_{\downarrow}(\boldsymbol{k},s) = P_{\leftarrow}(\boldsymbol{k},0)\,, \tag{A.4}$$

$$(s+\gamma)\tilde{P}_{\downarrow}(\boldsymbol{k},s) - \mathrm{i}k_y v_0 \tilde{P}_{\downarrow}(\boldsymbol{k},s) - \Gamma_1 \tilde{P}_{\leftarrow}(\boldsymbol{k},s) - \Gamma_2 \tilde{P}_{\uparrow}(\boldsymbol{k},s) - \Gamma_3 \tilde{P}_{\rightarrow}(\boldsymbol{k},s) = P_{\downarrow}(\boldsymbol{k},0)\,, \tag{A.5}$$

where the transforms are defined as

$$f(\boldsymbol{x},t) = \frac{1}{2\pi}\int_{-\infty}^{\infty} d\boldsymbol{k}\; f(\boldsymbol{k},t) e^{\mathrm{i}\boldsymbol{k}\cdot\boldsymbol{x}}\,, \tag{A.6}$$

$$f(\boldsymbol{x},t) = \int_{0}^{\infty} ds\; \tilde{f}(\boldsymbol{x},s) e^{st}\,. \tag{A.7}$$

To quantify $D_{\parallel}$, we ask how the total probability density $\tilde{P}(\boldsymbol{k},s) = \tilde{P}_{\rightarrow}(\boldsymbol{k},s) + \tilde{P}_{\uparrow}(\boldsymbol{k},s) + \tilde{P}_{\leftarrow}(\boldsymbol{k},s) + \tilde{P}_{\downarrow}(\boldsymbol{k},s)$ spreads out in time from a point, allowing us to calculate the mean-squared displacement. To this end, we specify the isotropic initial conditions $P_{\rightarrow}(\boldsymbol{k},0) = P_{\uparrow}(\boldsymbol{k},0) = P_{\leftarrow}(\boldsymbol{k},0) = P_{\downarrow}(\boldsymbol{k},0) = 1/4$ and consequently are free to choose any direction for $\boldsymbol{k}$. Arbitrarily setting $\boldsymbol{k} = k_x \hat{\boldsymbol{e}}_{\boldsymbol{x}}$ and solving algebraically yields

$$\tilde{P}(k_x,s) = \frac{2(2\gamma - 2\Gamma_2 + s)\big[(\Gamma_1-\Gamma_3)^2 + (\gamma+\Gamma_2+s)^2\big] + k_x^2 v_0^2(\gamma+\Gamma_2+s)}{2s(2\gamma-2\Gamma_2+s)\big[(\Gamma_1-\Gamma_3)^2+(\gamma+\Gamma_2+s)^2\big] + 2k_x^2 v_0^2\big[(\gamma+s)^2 - \Gamma_2^2\big]}\,. \tag{A.8}$$

We may then obtain the second moment of the probability density as

$$\langle \Delta\tilde{x}(s)^2\rangle = -\partial_{k_x}^2 \tilde{P}(k_x,s)\big|_{k_x=0} = \frac{v_0^2(\gamma+\Gamma_2+s)}{s^2\big[(\Gamma_1-\Gamma_3)^2+(\gamma+\Gamma_2+s)^2\big]}\,. \tag{A.9}$$

Taking the diffusive limit $s \to 0$ and performing the inverse Laplace transform (A.7) yields an expression for the diffusion coefficient $D_{\parallel}$ from the mean-squared displacement relation in the third equality of (13) in the main text:

$$\lim_{t\to\infty}\langle \Delta x(t)^2\rangle = 2D_{\parallel}t = \left(\frac{v_0^2(\gamma+\Gamma_2)}{(\Gamma_1-\Gamma_3)^2+(\gamma+\Gamma_2)^2}\right)t\,. \tag{A.10}$$

As noted in the main text, because the diffusion equation (3) does not involve $D_{\perp}$, the second moment of $P(x,y,t)$ does not contain any direct information about $D_{\perp}$. Instead, from the expansion described in (23)-(24), we may

consider the first moment when specifying both the initial position and initial velocity in equations (A.2)-(A.5). For example, to obtain $\langle x(t)\rangle_{\rightarrow}$ we set $P_{\rightarrow}(\boldsymbol{k},0) = 1$ and $P_{\uparrow}(\boldsymbol{k},0) = P_{\leftarrow}(\boldsymbol{k},0) = P_{\downarrow}(\boldsymbol{k},0) = 0$, and choose $\boldsymbol{k} = k_x\hat{\boldsymbol{e}}_{\boldsymbol{x}}$. Solving equations (A.2)-(A.5) as before and adding to obtain the total probability density yields

$$\tilde{P}(k_x,s) = \frac{(2\gamma - 2\Gamma_2 + s)\big[-\mathrm{i}k_x v_0(\gamma+\Gamma_2+s) + (\Gamma_1-\Gamma_3)^2 + (\gamma+\Gamma_2+s)^2\big]}{s(2\gamma-2\Gamma_2+s)\big[(\Gamma_1-\Gamma_3)^2+(\gamma+\Gamma_2+s)^2\big] + k_x^2 v_0^2\big[(\gamma+s)^2-\Gamma_2^2\big]}\,. \tag{A.11}$$

Note that, unlike in equation (A.8), $\tilde{P}(k_x,s)$ now has an imaginary part due to the asymmetry of the initial conditions. Differentiating in k_x obtains the first moment

$$\langle\tilde{x}(s)\rangle_{\rightarrow} = \mathrm{i}\partial_{k_x}\tilde{P}(k_x,s)\big|_{k_x=0} = \frac{v_0(s+\gamma+\Gamma_2)}{s\big[(s+\gamma+\Gamma_2)^2+(\Gamma_1-\Gamma_3)^2\big]}\,. \tag{A.12}$$

Taking the same approach but choosing instead $\boldsymbol{k} = k_y\hat{\boldsymbol{e}}_{\boldsymbol{y}}$, we find

$$\langle\tilde{y}(s)\rangle_{\rightarrow} = \mathrm{i}\partial_{k_y}\tilde{P}(k_y,s)\big|_{k_y=0} = \frac{v_0(\Gamma_1-\Gamma_3)}{s\big[(s+\gamma+\Gamma_2)^2+(\Gamma_1-\Gamma_3)^2\big]}\,. \tag{A.13}$$

Finally, introducing the notation $\omega = \Gamma_1-\Gamma_3$ and $\nu = \Gamma_1+2\Gamma_2+\Gamma_3$, and performing the inverse Laplace transform (A.7) on equations (A.12)-(A.13) leads to the logarithmic spiral form given in (25)-(26). The diffusion coefficients $D_{\parallel}$ and $D_{\perp}$ given in equations (27)-(28) then follow directly from the long-time response as $t\to\infty$.

One can understand the effect odd diffusivity may have on the concentration by constructing a boundary value problem. Let us consider a channel of length L whose top and bottom boundaries are impermeable and separated by a distance W, and to which particles are added at the left boundary and removed from the right boundary at a constant rate J_0W. These boundary conditions suggest the ansatz $\boldsymbol{J}(x,y) = J_0\hat{\boldsymbol{e}}_x$ for all (x,y). Then, from the constitutive relations of (1) and (2), we have

$$J_0 = -D_{\parallel}\partial_x C + D_{\perp}\partial_y C\,, \tag{A.14}$$

$$0 = -D_{\parallel}\partial_y C - D_{\perp}\partial_x C\,. \tag{A.15}$$

Upon defining the average concentration $C_0 = \frac{1}{LW}\int_0^L dx\int_0^W dy\; C(x,y) = C(0,0)$, equations (A.14)-(A.15) permit the solution

$$\begin{aligned} C^{\mathrm{ss}}(x,y) &= C_0 + \frac{J_0}{D_{\parallel}^2+D_{\perp}^2}\big(-D_{\parallel}x + D_{\perp}y\big) \\ &= C_0 + \frac{J_0}{v_0^2}\big(-\nu x + \omega y\big)\,. \end{aligned} \tag{A.16}$$

When $D_{\perp}\neq 0$, as seen from equation (A.16), asymmetric accumulation occurs along the impermeable channel walls giving rise to a linear concentration profile not only in the x-direction but in the y-direction as well.

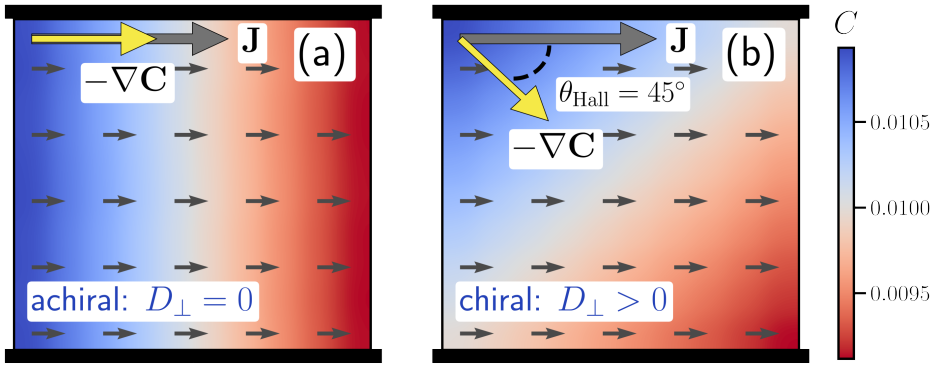

FIG. A.1. Steady-state concentration profile for diffusive flux through a channel with impermeable walls obtained from numerical simulation of the chiral random walk model without odd diffusivity (a; achiral, $\Gamma_1 = 1, \Gamma_2 = 0, \Gamma_3 = 1$) and with odd diffusivity (b; chiral, $\Gamma_1 = 1, \Gamma_2 = 0, \Gamma_3 = 0$).

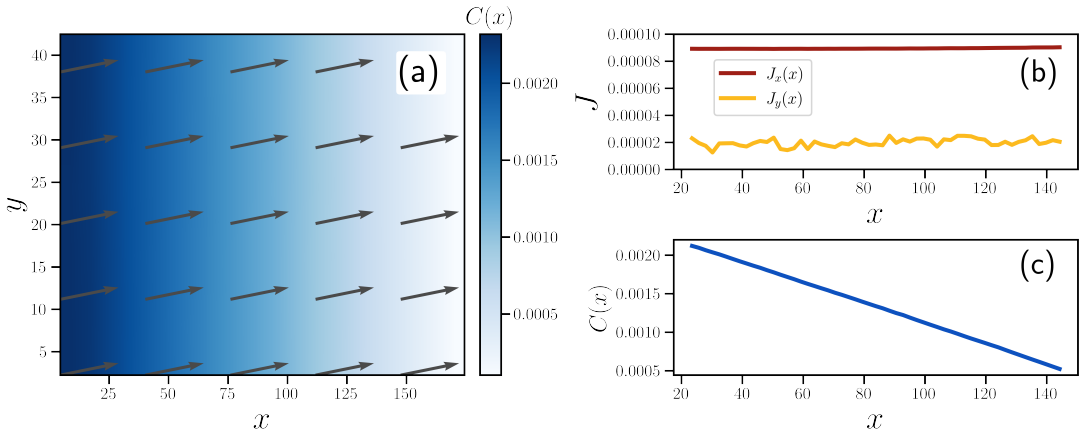

FIG. A.2. Results of a typical boundary-driven flux simulation of diffusion of a passive tracer particle in a chiral active bath. Parameters $\rho_{\text{active}} = 0.1$ and $\text{Pe} = 16$ have been chosen arbitrarily. (a) The flux field (arrows) is spatially homogeneous with a component in the y-direction due to odd diffusivity, while the concentration $C(x)$ varies linearly in the x-direction. The profiles of the flux and the concentration along the x-direction are plotted in (b) and (c), respectively. All quantities are averaged over 2×10^8 timesteps.

We check this solution by running numerical simulations of the chiral random walk model with corresponding boundary conditions, where the probability density P is interpreted as the concentration C. Specifically, we simulate the dynamics of a particle governed by equations (15)-(18) with either $\Gamma_1 = 1, \Gamma_2 = 0, \Gamma_3 = 1$ (left- and right-turning) or $\Gamma_1 = 1, \Gamma_2 = 0, \Gamma_3 = 0$ (left-turning only) for a single particle in a box of dimensions $L = 10$, $W = 10$, advancing the dynamics in timesteps of $\delta t = 0.01$. Whenever the particle crosses the boundary at $x = L$, it is replaced at $x = 0$ on the next timestep. In Figure A.1 we plot the steady-state simulation average, finding the resulting flux field to be uniform while the concentration field depends linearly on x and y, in agreement with equation (A.16) where $C_0 = 0.01$ and $J_0 = 0.0001$.

A.2. MOLECULAR DYNAMICS SIMULATION DETAILS

Molecular dynamics simulations of a passive tracer particle diffusing in a chiral active bath composed of self-spinning dumbbells were performed in LAMMPS [1] with custom modifications[1] implementing the microscopic active forces and constant-flux boundary conditions. The nonconservative active force $\boldsymbol{f}_i^A$ in equation (29) affects only the dumbbell particles, with constant magnitude $|\boldsymbol{f}_i^A| = f^A$. The orientation of $\boldsymbol{f}_i^A$ is perpendicular to the bond vector $\boldsymbol{r}_i - \boldsymbol{r}_j$ for the bonded pair i and j, and directed oppositely ($\boldsymbol{f}_i^A = -\boldsymbol{f}_j^A$), inducing rotation of the dumbbell. Chiral active dumbbells are composed of two particles held together by a harmonic potential $U^{\text{Harm}}(r) = \frac{1}{2}k(r - r_0)^2$, where r is the separation distance. We set the spring constant $k = 100$ and the reference bond length $r_0 = 1$. All particles (including the passive tracer) interact with non-bonded neighbors through a Weeks-Chandler-Andersen [2] potential defined by

$$U^{\text{WCA}}(r) = \begin{cases} 4\epsilon\left[(\sigma/r)^{12} - (\sigma/r)^{6}\right] + \epsilon & r < 2^{1/6}\sigma \\ 0 & r \geq 2^{1/6}\sigma\,, \end{cases} \tag{A.17}$$

such that $U = U^{\text{Harm}} + U^{\text{WCA}}$ in equation (29). Here, m, σ and ϵ are the particle mass, diameter and interaction energy, providing characteristic mass, length and energy scales which define the Lennard-Jones units system. All simulation results are reported in Lennard-Jones units. The Langevin dynamics described in equation (29) were discretized with a velocity Verlet scheme with time step $\delta t = 0.005$ and bath temperature $k_{\text{B}}T = 1.0$. The friction coefficient was set to $\zeta = 2.0$ for dumbbell particles and $\zeta = 0$ for the passive tracer particles, such that the tracers move ballistically between collisions. Simulations were performed at high dilution of the passive solute particles, where

[1] Our simulation and analysis code is publicly available at https://github.com/mandadapu-group/active-matter.

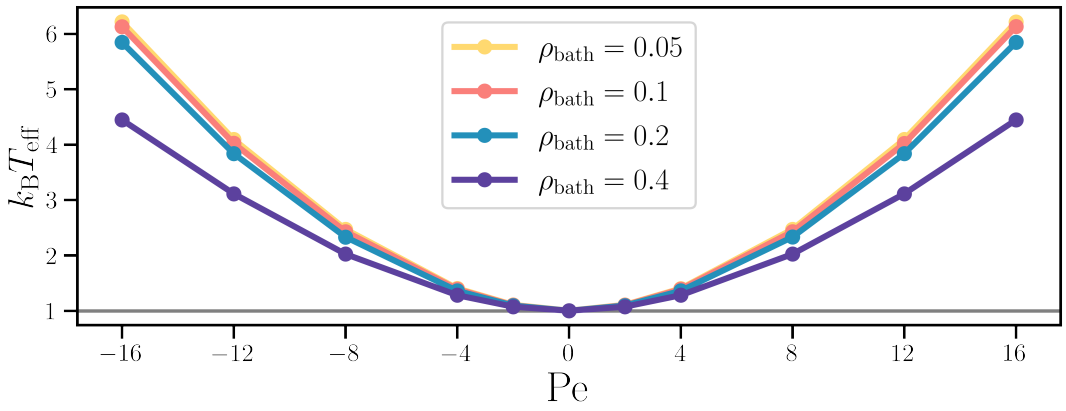

FIG. A.3. Effective kinetic temperature of the passive tracer particle across all values of ρ_{bath} and Pe corresponding to the simulation results displayed in Figure 3 of the main text.

all simulations contained at least twenty times the number of active dumbbell solvent particles as passive tracer solute particles.

Calculation of the velocity autocorrelation tensor entering the Green-Kubo relations (13) and (14) was performed in a fully periodic system in a non-equilibrium steady state exhibiting stationarity and spatial homogeneity of all observables. Boundary-driven flux simulations were performed in a rectangular simulation box with special boundary conditions affecting the diffusing passive solute particles but not the active bath particles. A passive solute particle passing out of the simulation box through the right boundary behaves periodically, reappearing at the left boundary. A passive solute particle particle passing through the left boundary is reflected back into the simulation box. All interactions across the boundaries remain fully periodic. These conditions ensure a constant flux of particles across the simulation box, with the concentration varying linearly in x, as shown in Figure A.2 for a particular simulation with $\rho_{\mathrm{active}} = 0.1$ and $\mathrm{Pe} = 16$.

A.3. LINEAR RESPONSE MOBILITY TENSOR

The mobility tensor $\boldsymbol{\mu}$ provides a linear relation between a particle's drift velocity $\boldsymbol{u}$ and an applied body force $\boldsymbol{g}$ which, within the context of linear response theory, is expected to be valid for sufficiently small $\boldsymbol{g}$

$$u_i = \mu_{ij} g_j \,. \tag{A.18}$$

For passive systems, the mobility and diffusivity are ordinarily connected by the Einstein relation

$$D_{ij} = k_{\mathrm{B}} T \mu_{ij} \,. \tag{A.19}$$

Active matter systems need not obey such a relation. Indeed, one of the hallmarks of many active matter models is the "enhancement" of the diffusivity, due to the presence of active driving forces, over its value in the absence of such forces. When such behavior is present, the Green-Kubo relations for the diffusivity coefficients in equations (13)-(14) are expected to remain valid while predictions of the diffusivity coefficients from linear response theory *via* the Einstein relation (A.19) cease to be applicable.

To illustrate this, let us briefly consider a simple model system which exhibits nonzero odd diffusivity but whose mobility tensor contains no antisymmetric part. Namely, we consider an active Brownian particle in two dimensions in the overdamped regime, driven by internally-generated forces oriented along a director $\hat{\boldsymbol{u}}(t) = \big(\cos\theta(t),\ \sin\theta(t)\big)$, where $\theta(t)$ is the polar angle of the director. We consider the case where the evolution of the director has both a random part, due to interactions with the environment or internal noise, as well as a deterministic bias, due to an internally generated torque. This setup has been suggested as a minimal model for zooplankton such as *Daphnia*, which tend to steer either left or right as they swim in-plane [3, 4]. The Langevin equations for such a system are

$$\dot{\boldsymbol{r}} = v_0 \hat{\boldsymbol{u}} \,, \tag{A.20}$$

$$\dot{\theta} = \omega_0 + \sqrt{2D_r}\xi_r(t) \,, \tag{A.21}$$

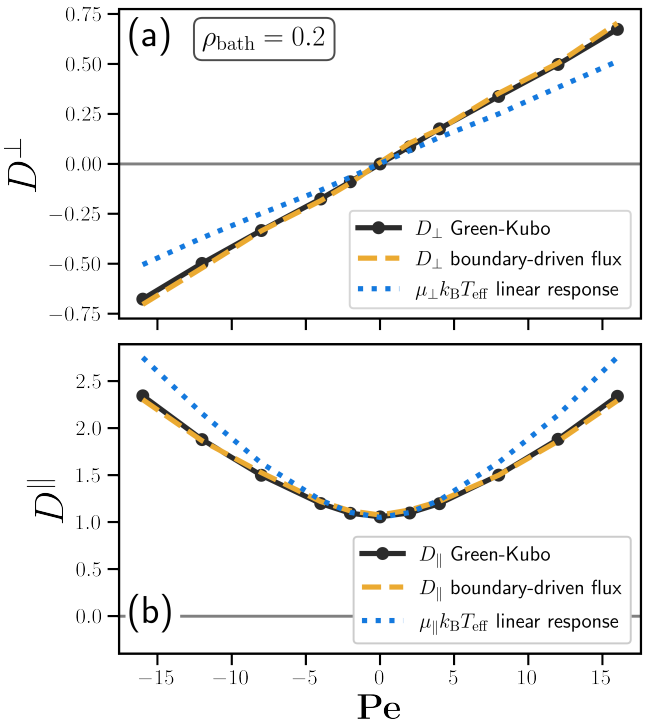

FIG. A.4. Comparison of the diffusion coefficients for a passive tracer particle in an active dumbbell bath with $\rho_{\text{bath}} = 0.2$ obtained from Green-Kubo and boundary-driven flux calculations (solid lines and dashed lines, respectively) against those predicted from the from the mobility using the Einstein relation with an effective kinetic temperature.

where $\xi_r(t)$ is Gaussian white noise characterized by $\langle \xi_r(t) \rangle = 0$ and $\langle \xi_r(t) \xi_r(t') \rangle = \delta(t - t')$.

The velocity correlation functions for this isotropic system are

$$\langle v_x(t) v_x(0) \rangle = \langle v_y(t) v_y(0) \rangle = v_0^2 \langle \cos\theta(t) \cos\theta(0) \rangle \tag{A.22}$$

$$\langle v_x(t) v_y(0) \rangle = -\langle v_y(t) v_x(0) \rangle = v_0^2 \langle \cos\theta(t) \sin\theta(0) \rangle \tag{A.23}$$

Using trigonometric product identities, one may show that

$$\langle \cos\theta(t) \cos\theta(0) \rangle = \frac{1}{2} \langle \cos\big(\theta(t) - \theta(0)\big) + \cos\big(\theta(t) + \theta(0)\big) \rangle = \frac{1}{2} \langle \cos\phi(t) \rangle \tag{A.24}$$

$$\langle \cos\theta(t) \sin\theta(0) \rangle = \frac{1}{2} \langle \sin\big(\theta(t) + \theta(0)\big) - \sin\big(\theta(t) - \theta(0)\big) \rangle = -\frac{1}{2} \langle \sin\phi(t) \rangle \tag{A.25}$$

where the second equality in both equations follows from isotropy and $\phi(t) = \theta(t) - \theta(0)$ is the displacement at time t of the angle from its initial value.

The Fokker-Planck equation corresponding to the Langevin equation (A.21) is [5]

$$\frac{\partial}{\partial t} f(\phi, t) = \omega_0 \frac{\partial}{\partial \phi} f(\phi, t) + D_r \frac{\partial^2}{\partial \phi^2} f(\phi, t)\,, \tag{A.26}$$

where $f(\phi, t)$ is the probability density of the director angle. Defining the characteristic function of the angle distribution as

$$\tilde{f}(k, t) = \langle e^{\mathrm{i}k\phi} \rangle = \int_{-\infty}^{\infty} d\phi \; e^{\mathrm{i}k\phi} f(\phi, t)\,, \tag{A.27}$$

Equation (A.26) can be solved in Fourier space resulting in

$$\tilde{f}(k, t) = \exp\left[(\mathrm{i}k\omega_0 - k^2 D_r)t\right]. \tag{A.28}$$

Thus,

$$\langle \cos\phi(t)\rangle = \mathrm{Re}\,\tilde{f}(1,t) = \cos(\omega_0 t)e^{-D_r t}\,, \tag{A.29}$$

$$\langle \sin\phi(t)\rangle = \mathrm{Im}\,\tilde{f}(1,t) = \sin(\omega_0 t)e^{-D_r t} \tag{A.30}$$

Finally, inserting equations (A.24)-(A.25) and (A.29)-(A.30) into the Green-Kubo relations (13)-(14) yields

$$D_\parallel = \frac{v_0^2}{2}\frac{D_r}{D_r^2+\omega_0^2}\,, \tag{A.31}$$

$$D_\perp = \frac{v_0^2}{2}\frac{\omega_0}{D_r^2+\omega_0^2}\,. \tag{A.32}$$

Note that the functional form is identical to that of the chiral random walk model in equations (27)-(28), elucidating the merits of this model in capturing the essential features of the odd diffusivity. Now, as the mechanisms generating active propulsive forces and steering torques were assumed to be "internal", *i.e.* not resulting from external interactions, the mobility tensor in this idealized model will be symmetric and independent of the values of v_0 and ω_0, for instance following Stokes' Law.

We now evaluate the applicability of an effective Einstein relation for the chiral active dumbbell bath model discussed in the main text, upon defining an effective temperature computed from the mean kinetic energy of the diffusing passive tracer particle (A.19):

$$k_\mathrm{B}T_\mathrm{eff} = \frac{1}{2}\langle|\boldsymbol{v}_\mathrm{tracer}|^2\rangle\,. \tag{A.33}$$

The dependence of this temperature on Pe is plotted for all densities of the dumbbell bath in Figure A.3, corresponding to the simulation results plotted in Figure 3 of the main text. The temperature of the nonequilibrium stationary state is determined by the competition between active forces and dissipative Langevin forces and, more noticeably at higher dumbbell densities, collisions occurring between dumbbells.

The resulting relationship is plotted in Figure A.4, where we have defined the isotropic mobility tensor analogously to the diffusivity as $\mu_{ij} = \mu_\parallel\delta_{ij} - \mu_\perp\epsilon_{ij}$. We observe that the linear response prediction captures only the qualitative behavior of $D_\perp$ and $D_\parallel$, with the disagreement most pronounced at high Pe. Note, finally, that because the sign of the linear response error differs for $D_\perp$ and $D_\parallel$ in Figure A.4, no single choice of T_eff could simultaneously reconcile the disagreement for both diffusion coefficients.

[1] S. J. Plimpton, Journal of computational physics **117**, 1 (1995), see also http://lammps.sandia.gov/.
[2] J. D. Weeks, D. Chandler, and H. C. Andersen, The journal of chemical physics **54**, 5237 (1971).
[3] P. Romanczuk, M. Bär, W. Ebeling, B. Lindner, and L. Schimansky-Geier, Eur. Phys. J. S.T. **202**, 1 (2012).
[4] N. Komin, U. Erdmann, and L. Schimansky-Geier, Fluctuation and Noise Letters **4**, 151 (2004).
[5] Hannes Risken, *The Fokker-Planck Equation*, 2nd ed. (Springer, 1989).